Optimization of PES/ZnO mixed matrix membrane preparation using response surface methodology for humic acid removal

Abdul Latif Ahmad[*,**,†], **Abdullah Adnan Abdulkarim**[*,***], **Suzylawati Ismail**[*], and **Ooi Boon Seng**[*]

*School of Chemical Engineering, Engineering Campus, Universiti Sains Malaysia, 14300, Nibong Tebal, Penang, Malaysia
**Geology and Geophysics Department, Faculty of Science, King Saud University, P. O. Box 2455, Riyadh 11451, Saudi Arabia
***Chemical and Petrochemical Research Center, Commission for Research and Industrial Development, Ministry of Industry and Minerals, Baghdad, Iraq

Abstract−The application of response surface methodology (RSM) in preparation and optimization of membranes is important in order to reduce the effort and time needed to achieving an optimum performance. RSM was used to develop an optimum polyethersulfone (PES)/ZnO mixed matrix (MM) membrane for humic acid removal. The MMs were synthesized by dispersing various amounts of hydrophilic ZnO nanoparticles (NPs) into a solution containing PES, polyvinylpyrrolidone (PVP) and dimethylacetamide (DMAc). Flat sheet MM membranes were prepared via the phase inversion method using the central composite design (CCD). The effects of four preparation parameters, such as PES, ZnO, PVP weight percentages and solvent evaporation time, were investigated. Pure water flux (PWF), humic acid flux (HAF) and humic acid rejection (HAR) were selected as a model responses. It was shown that PES and PVP were mainly affected on both PWF and HAF. Furthermore, the interaction effect between PES and ZnO-NPs shows a significant effect on PWF, while the quadratic effects of both solvent's evaporation time and ZnO-NPs weight percentage coupled with the interaction effect between PES and PVP weight percentage shows the most significant parameters that affects HAR. The optimization method was subjected to maximize all of the PWF, HAF and HAR. It was also determined that the optimized membrane can be synthesized from a solution containing 17.25 wt% PES, 3.62 wt% ZnO and 3.75 wt% PVP with 15 s of solvent evaporation time. The optimum values of PWF, HAF and HAR were 222.3 (L/m² h), 94.7 (L/m² h), and 96.34%, respectively. Thus, it can be concluded that the CCD technique is capable of optimizing PES-ZnO membrane performance.

Keywords: Mixed Matrix Membrane, Zinc Oxide Nanoparticles, Humic Acid, Central Composite Design

INTRODUCTION

The increasing depletion of water resources demands an alternative technique for water recycling. One of the most important concerns is in the production of high-quality drinking water. It is well established that the presence of natural organic matter (NOM) in aquatic resources is not harmful, but can become a threat if water is treated with chlorine in the disinfection stage. The presence of organic matter, such as humic acid (HA), can lead to the formation of chlorinated by-products in drinking water via the reaction of chlorine with organic compounds [1]. Recently, research into membrane processes for the purification of drinking water has been forthcoming. Utilizing membranes in the separation of pollutants from water is particularly attractive due to their high separation efficiencies with a stable production of high water quality [2]. There are various advantages in the use of membrane technology for the purification of water, such as high efficiency, low cost and lack of secondary pollution.

Polyethersulfone (PES) is one of the polymeric materials widely used for membrane fabrication because of its high mechanical strength, good heat and aging resistance, and high chemical stability [3]. These advantages promote the frequent use of PES membranes in several fields, such as in water or wastewater treatment [4]. However, PES membranes are prone to fouling because of their high hydrophobicity, thus preventing their long-term use. A common technique often used for overcoming the fouling effect involves the incorporation of hydrophilic additives within the membrane structure. The addition of hydrophilic additives to PES membranes generates a surface that is more resistant to fouling [5].

Various investigations found in the literature used additives in the modification of PES [6,7]; hence it seems to be the easiest technique to enhance the PES membrane for its long time stability and industrial application [8,9]. The incorporation of inorganic materials in PES membranes has been extensively studied, and the effects of these additives on the membrane efficiency have been reported [10-14]. Due to the high mechanical strength and thermal properties of these particles, they can improve the structure as well as the performance of PES membranes [15].

Zinc oxide nanoparticles (ZnO-NPs) have received significant attention due to low cost, high surface area, photocatalytic activity and anti-bacterial properties [16,17]. ZnO-NPs have been used with different membrane materials and this has led to an improved performance [13,18-23]. Wang et al. [18] improved cellulose acetate membranes using ZnO-NPs (4 wt%), which led to an enhance-

†To whom correspondence should be addressed.
E-mail: chlatif@usm.my, masterchem76@yahoo.com

ment of 111.1% of the flux compared to pristine membranes. Leo et al. [22] improved the hydrophilicity of the polysulfone (PS) membrane by incorporating ZnO-NPs (in the range of 1-4 wt%) with polyvinyl alcohol as a dispersion agent, which yielded a 12-fold improvement in membrane permeability due to the presence of ZnO-NPs (2 wt%) in the PS membrane. Additionally, this membrane had the highest fouling resistance during oleic acid filtration. Balta et al. [13] used high PES concentrations over a wide range of ZnO-NPs concentrations (0.035-4 wt%) to develop a mixed matrix (MM) membrane. They found a significant improvement in the water permeability as well as in the HA rejection. However, at high polymer concentrations, the composite membrane shows a reduction in permeability due to a drop in the NP dispersion rate. Shen and co-workers [19] dispersed ZnO-NPs in a solvent with a low concentration of PES (16 wt%) and polyethylene glycol (PEG). Their results revealed that the membrane hydrophilicity increased with increasing ZnO concentration, while the flux shows an improvement of 254% (obtained at 0.398 wt% ZnO-NPs) relative to the pristine PES membrane. In our previous work, [23] where ZnO was incorporated in PES matrix using PVP as a dispersion agent, the membrane flux and rejection were improved by the addition of ZnO-NPs in PES matrix.

Many researchers have tried to enhance and optimize membrane morphology and performance using a statistical approach [24-29]. Statistical approaches like response surface methodology (RSM) have been widely used to calculate the complex interactions between the independent process parameters. The application of statistical analysis seems more practical for investigating the effects of the variables involved in membrane formation, especially when more than one additive is added into the solution because the membrane formation parameters are related to each other in such a complicated system. However, to the authors' best knowledge, RSM has never been applied to optimize the preparation parameters of PES/ZnO membrane. Therefore, our objective was to optimize the PES, ZnO-NPs and PVP content as well as the solvent evaporation time. The interactions between the preparation parameters were examined using central composite design (CCD), while the optimization conditions were subjected to maximizing the pure water flux (PWF), humic acid flux (HAF) and humic acid rejection (HAR). PWF, HAF and HAR were selected because they were the most important parameters for membrane performance in the filtration of HA solutions.

MATERIALS AND METHODS

1. Materials

Polyethersulfone (PES Ultrason E6020P with Mw=58,000 g/mol) was supplied by BASF. Polyvinylpyrrolidone (PVP) (with Mw= 40,000 g/mol), sodium hydroxide, humic acid and N,N-dimethylacetamide (DMAc) as a solvent were supplied by Sigma Aldrich, USA. A commercial form of zinc oxide nanoparticles, ZnO (particle size ranges from 10-30 nm) nanopowder (purity >99%) was supplied by US Research Nanomaterials, Inc. 3302 Twig Leaf Lane.

2. Membrane Preparations

The membrane solutions were prepared by dispersing varying amounts of ZnO-NPs (ranging from 0 to 5 wt%) into the corre-

sponding volume of DMAc. The solution was mechanically stirred (600 rpm) at room temperature for 3 h. The resulted mixture was ultrasonicated for 15 min using ultrasonic probe (frequency equal to1) and stirred for another 3 h. The implementation of probe or direct sonication was found to be efficient in increasing the dispersions of nanoparticles [30]. Also, this technique was recently used in preparation of mixed matrix membranes [31]. Furthermore, a predetermined amount of PVP (ranging from 0 to 5 wt%) was added and stirred continuously for another 5 h. Then, a corresponding amount of PES polymer (ranging from 15 to 18 wt%) was added and the solution was kept under mechanical stirring (500 rpm) at 60 $^{\circ}$C for 24 h. For the removal of the bubbles, the homogeneous polymeric solution was placed in an ultrasonic bath for 3 h. The polymeric solution was cast with a 200 μm-thick casting knife onto a glass plate using a filmograph (K4340 automatic Film Applicator, Elcometer) in an inert atmosphere. Then, the membrane was exposed to air (ranging from 0 to 60 s) and subsequently moved to a non-solvent bath (containing distilled water) at 20 $^{\circ}$C and left for 24 h for precipitation. The acquired membranes were thoroughly washed with distilled water, left in distilled water for one day to ensure a complete removal of solvent and was later stored wet.

3. Design of Experiments

A set of 30 experiments were designed based on CCD to prepare the PES/ZnO MM flat sheet membranes using the phase inversion method. CCD is the most accepted second-order regression model used in the RSM [32] due to its efficiency with respect to the number of runs required for fitting a second order response surface model. In addition, CCD is ideal for sequential experimentation, as well as allows a reasonable amount of information to test for lack of fit and does not involve an unusual large number of design points [33].

The RSM was used to optimize the final membrane performance. Four independent variables, PES wt%, ZnO wt%, PVP wt% and solvent evaporation time, were investigated. The CCD consists of five levels, as well as sixteen factorial points, eight axial points and six central points. The selection of levels for the independent variables was based on a study reported elsewhere [34] and some preliminary experiments. The experiments were designed to inspect the linear, quadratic and cross-products of the membrane preparation variables. The range and levels of the independent variables investigated are listed in Table 1. According to the CCD, each variable used at five different levels was coded as $-\alpha$, -1, 0, $+1$ and $+\alpha$. All variables at the zero level correspond to the center points; and the combination of each of these variables either at their lowest level ($-\alpha$) or highest level ($+\alpha$) with the other variables at the zero level corresponds to the axial points. The output of α depends on the number of variables (n). For instance, if n=4, $\alpha=\sqrt{n}=2$. The experimental set and the model responses (PWF, HAF, and HAR) are listed in Table 2.

4. Statistical Analysis Using Design of Experiments

Regression analysis and analysis of variance (ANOVA) involved using the design-expert software version 6.06 (State Ease Inc., Minneapolis, USA). The experimental responses (PWF, HAF and HAR) were analyzed via RSM using the quadratic equation. The regression method used for this model is considered helpful when one or more factors in the experiment are quantitative [35]. A

Table 1. Input variables and their respective levels employed by DOE

Variable	Coding	Unit	Level				
			$-2(-\alpha)$	-1	0	1	$2(+\alpha)$
PES	A	Wt%	15	15.75	16.5	17.25	18
ZnO	B	Wt%	0	1.25	2.5	3.75	5
PVP	C	Wt%	0	1.25	2.5	3.75	5
Time	D	s	0	15	30	45	60

regression was performed to describe the data collected, whereby an observed response was based approximately on a functional relationship between the estimated response and to one or more of the input variables. The regression model of four-factor factorial experiment can be written as:

$$y=\beta_0+\beta_1X_1+\beta_2X_2+\beta_3X_3+\beta_4X_4+\beta_{11}X_1^2+\beta_{22}X_2^2+\beta_{33}X_3^2+\beta_{44}X_4^2$$
$$+\beta_{12}X_1X_2+\beta_{13}X_1X_3+\beta_{14}X_1X_4+\beta_{23}X_2X_3+\beta_{24}X_2X_4+\beta_{34}X_3X_4 \qquad (1)$$

where y is the response; βs are the parameters whose values are to be determined; X_1 is a variable that represents factor A; X_2 is the variable that represents factor B, X_3 is the variable that represents factor C; X_4 is the variable that represents factor D; X_1X_2, X_1X_3, X_1X_4, X_2X_3, X_2X_4 and X_3X_4 represents the interactions between the variables. There were four manipulated variables taken into account in this study: the PES weight percentage (A), ZnO weight percentage (B), PVP weight percentage (C), and solvent evaporation time (D). It was easier to utilize second-order terms instead of third-order terms in the development of the regression model.

The RSM from the design expert software was used to obtain the best model for three response functions (PWF, HAF, and HAR). A regression analysis was performed to fit the response functions and predict the outcome of these responses. The result of the full-factorial was performed to find the possible interactions between the input variables (PES, ZnO, PVP weight percentage and the solvent evaporation time). The investigation of the interactions between these parameters led to the desired membrane performance as a function of the input parameters. Tests for the significance of the regression model and the model coefficients were also performed. The p-value is the probability of obtaining a test statistic at least, as extreme as the one that was actually observed, assuming that the null hypothesis is found true. Normally, the null hypothesis is rejected when the p-value turns out to be less than a certain significance level, usually 0.05 or 0.01. Such result would indicate that the observed result would be unlikely enough relative to the null hypothesis. Additionally, when the confidence level is 95%, it is considered significant [36]. This probability corresponds to p-value of less than 0.05, and the model is significant [37]. Conversely, the F-value refers to the ratio of explained to unexplained variances and always has a value greater than one.

5. Characterization of the Membrane

Membrane flux and the separation performance measurements of the prepared membranes were performed in a cross-flow filtration setup as shown in Fig. 1. All experiments were performed at the ambient laboratory temperature of $22\pm1\,^{\circ}C$. Typically, the experiments were conducted using a cross-flow cell with an effective membrane area of 41 cm^2 and a constant cross flow rate of
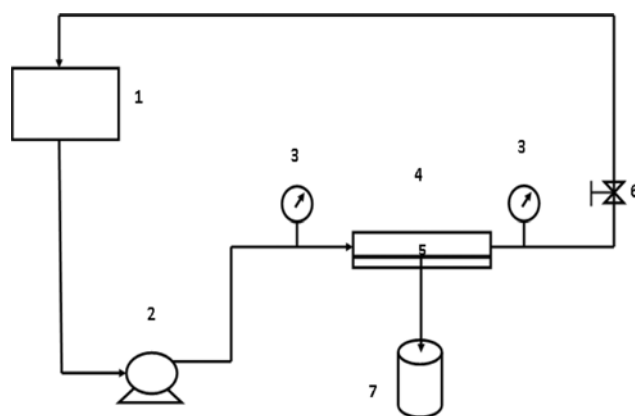
Fig. 1. Schematic diagram of the cross-flow unit.
1. Feed tank
2. Peristaltic pump
3. Pressure gauge
4. Cross-flow cell
5. Membrane
6. Control valve
7. Permeate

1,000 ml/min (equal to 18.93 cm/s of cross flow speed inside the testing cell) using a Flex-Pro-A4V peristaltic metering pump (Blue-White, USA). Initially, each of the tested membranes were compressed with pure water at 150 kPa for 1 h. The PWF was performed at 100 kPa and measured after 60 min of water filtration. A 5 L feed solution containing (10 mg/L, pH=7.7) of the HA solution was prepared and re-circulated at 100 kPa through the aforementioned cell. The HA solution was used to investigate the membrane rejection and fouling. The HA concentration in the permeate was recorded after 60 min of filtration (full recycling of both the permeate and retentate), excluding the flux sampling.

The PWF (J_{WF}) was computed according to the following equation:

$$J_{WF}=\frac{V}{A*t} \qquad (2)$$

where J_{WF} is the PWF (L/m^2 h), V refers to the permeate volume (L), A is the effective membrane surface area (m^2) and t is the measurement time (h). The HA concentrations in the feed and permeate fluxes were determined using a UV-visible spectrophotometer (Pharo 300, Merck-Germany) at a wavelength of 254 nm. The membrane rejection was calculated according to Eq. (3):

$$Rejection=\left(1-\frac{C_p}{C_f}\right)\times100\% \qquad (3)$$

where C_p (mg/L) and C_f (mg/L) represents the solute concentrations in the permeate and feed, respectively.

The pore sizes of the membranes were determined using a gas flow/liquid displacement method with a capillary flow Porometer Porolux 1000 (Benelux Scientific, Belgium). Prior to the test, membrane samples having a diameter of 10 mm were immersed in perfluoroethers (for 5 min) and then characterized using the "dry up-wet up" method. The mean pore size was then determined using LabView software.

The surface morphologies and the cross sectional area of the prepared PES/ZnO membranes were studied using scanning electron microscopy (SEM) on a HITACHI tabletop microscope (TM-3000-Japan) operated at 15 kV. The membrane samples were cut into small sizes and mounted on double-sided carbon adhesive foil as the sample holder. Prior to the SEM test, sputter coating was used (Quorum-SC7620) to coat the membrane surface and cross sectional area with a thin layer of gold to avoid electrostatic charging.

Table 2. Experimental responses under different experimental conditions

Std.	Run	PES (wt%)	ZnO (wt%)	PVP (wt%)	Time (s)	PWF (L/m^2 h)	HAF (L/m^2 h)	Rejection (%)
1	14	15.75	1.25	1.25	15	150	60	94.66
2	29	17.25	1.25	1.25	15	23	19.05	95.5
3	11	15.75	3.75	1.25	15	85.71	55	97.8
4	3	17.25	3.75	1.25	15	26	20	94.27
5	1	15.75	1.25	3.75	15	320	122	93.03
6	12	17.25	1.25	3.75	15	295	140	93.55
7	16	15.75	3.75	3.75	15	308	110	94.73
8	8	17.25	3.75	3.75	15	200	66	97.98
9	19	15.75	1.25	1.25	45	240	100	97.2
10	27	17.25	1.25	1.25	45	45.83	31.17	95.82
11	13	15.75	3.75	1.25	45	75	52	98.1
12	26	17.25	3.75	1.25	45	34.28	29	93.65
13	30	15.75	1.25	3.75	45	360	155	95
14	18	17.25	1.25	3.75	45	47	40	94.27
15	2	15.75	3.75	3.75	45	248	160	94.27
16	23	17.25	3.75	3.75	45	295.55	115	97.37
17	5	15	2.5	2.5	30	346	115	94.27
18	7	18	2.5	2.5	30	40	22	96.75
19	15	16.5	0	2.5	30	250	120	88
20	10	16.5	5	2.5	30	161.72	111.31	91.48
21	9	16.5	2.5	0	30	13.19	11.43	96.13
22	25	16.5	2.5	5	30	535.69	145	93.65
23	24	16.5	2.5	2.5	0	153.05	85	97.98
24	28	16.5	2.5	2.5	60	209.05	111.31	96.2
25	21	16.5	2.5	2.5	30	184	87	93.7
26	4	16.5	2.5	2.5	30	100	73	93
27	17	16.5	2.5	2.5	30	171.4	104.5	92.5
28	6	16.5	2.5	2.5	30	124	70	94.58
29	22	16.5	2.5	2.5	30	184	88	94.58
30	20	16.5	2.5	2.5	30	186	89	95

Table 3. ANOVA results of three responses (PWF, HAF and HAR)

Resp.	Equation	R^2	Sign. terms (actual)	Sign. terms (coded)
PWF	$2692.2 - 162.6 * PES - 560.9 * ZnO + 81.2 * PVP + 33.2 * PES * ZnO$	74.44	PES, PVP, PES $*$ ZnO	A, C, A $*$ B
HAF	$510.9 - 29.9 * PES + 26.9 * PVP$	73.68	PES, PVP	A, C
HAR	$421.5 - 37.1 * PES + 3.2 * ZnO - 17.9 * PVP - 0.262 * Time + 1.05 * (PES)^2$ $- 0.542 * (ZnO)^2 + 0.281 * (PVP)^2 + 0.0043 * (Time)^2 + 0.977 * PES * PVP$	71.23	Time^2, ZnO^2, (PES $*$ PVP), ZnO, PES^2	D^2, B^2, A $*$ C, B, A^2

RESULT AND DISCUSSION

1. Regression Analysis and ANOVA Results

The experiments and the response values are shown in Table 2. The PWF ranges from 13.19 to 535.69 (L/m^2 h), while the HAF and HAR ranges from 11.43 to 160 (L/m^2 h) and from 88 to 98.1%, respectively. The experimental error was obtained using runs 4, 6, 17, 20-22.

The ANOVA results for the three responses are shown in Table 3. The second-order model was used to fit the experimental results. The P-values for all three models were found to be statistically significant at p<0.05, and the lack of fit was found to be insignificant at p>0.05.

The parameters that show significant effects on PWF were PES, PVP and likewise the interaction effect between PES and ZnO. The significance of the models for PWF was in the order of C>A>AB. Moreover, PES and PVP weight percentages show significant model terms for HAF response, and the significance of the models for HAF was in the order of C>A. The significant parameters for HAR response were expressed by both the first- and second-order effects, where the parameter that has a first-order effect on the HAR was the ZnO weight percentage. The quadratic effects of the parameters were expressed by the PES and ZnO weight

percentages as well as the solvent evaporation time. In addition, the interaction of the PES and PVP weight percentages (AC) also shows a significant model term, where the F-value was less than 0.05. The significance of the preparation parameters for HAR was in the order of D^2>B^2>AC>B>A^2.

Note that the insignificant model parameter for PWF (B) and HAR (A, B, C, D) cannot be removed from the model equations to maintain models hierarchy. Also, the first-order term of the solvent evaporation time (D) parameter is not significant in all three responses (PWF, HAF and HAR). However, the quadratic effect of solvent evaporation time (D^2) was found to be the most significant parameter of HAR response. Among many membrane performance parameters, the HAF was chosen as humic acid, and has been widely used as a model for organic foulants in aqueous solutions [38]. Thus, it gives an indication of the membrane efficacy during the filtration process.

The PWF, HAF and HAR predicted by the models were compared with the experimental data in Fig. 2, which indicates that the experimental data were satisfactorily fitted using equations listed in Table 3.

2. PWF and HAF Responses

In the present work, the polymeric dope solution contains two additives, ZnO-NPs and PVP. So, it was important to investigate
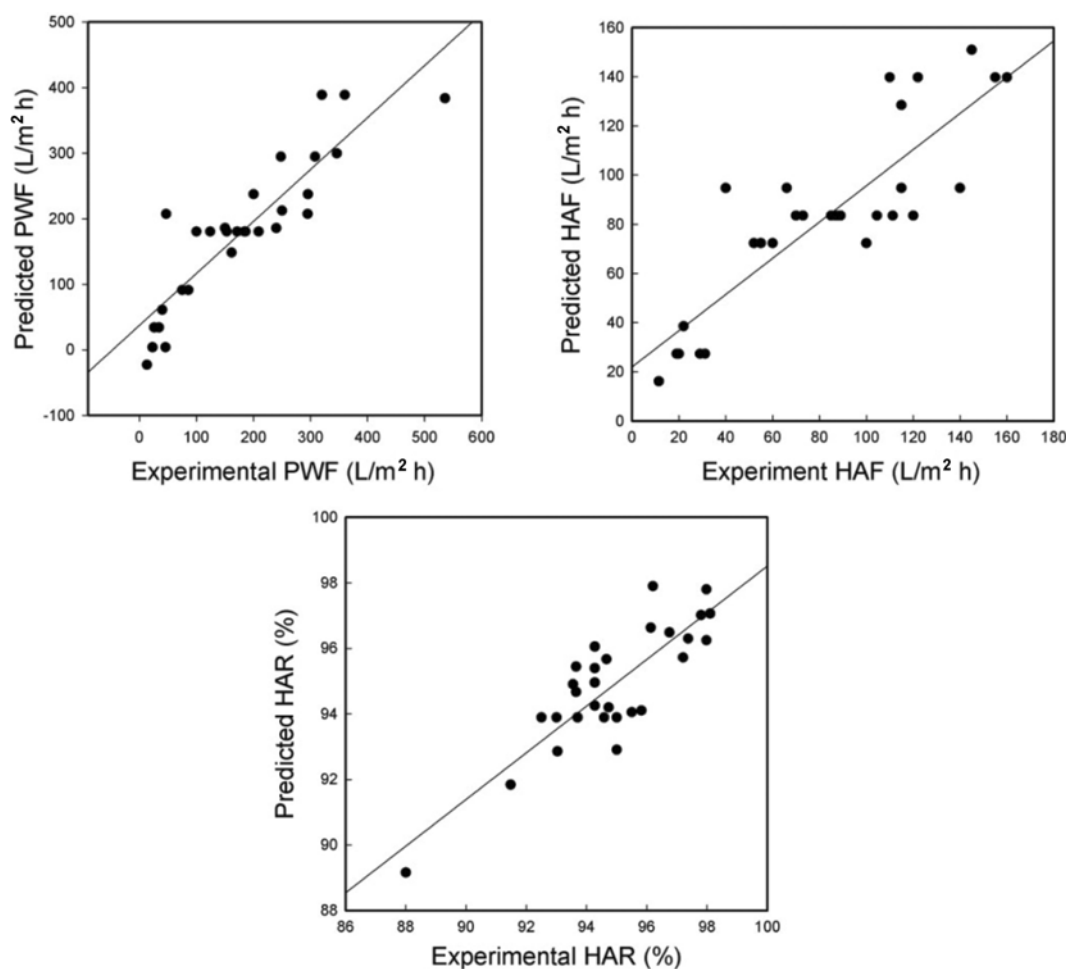

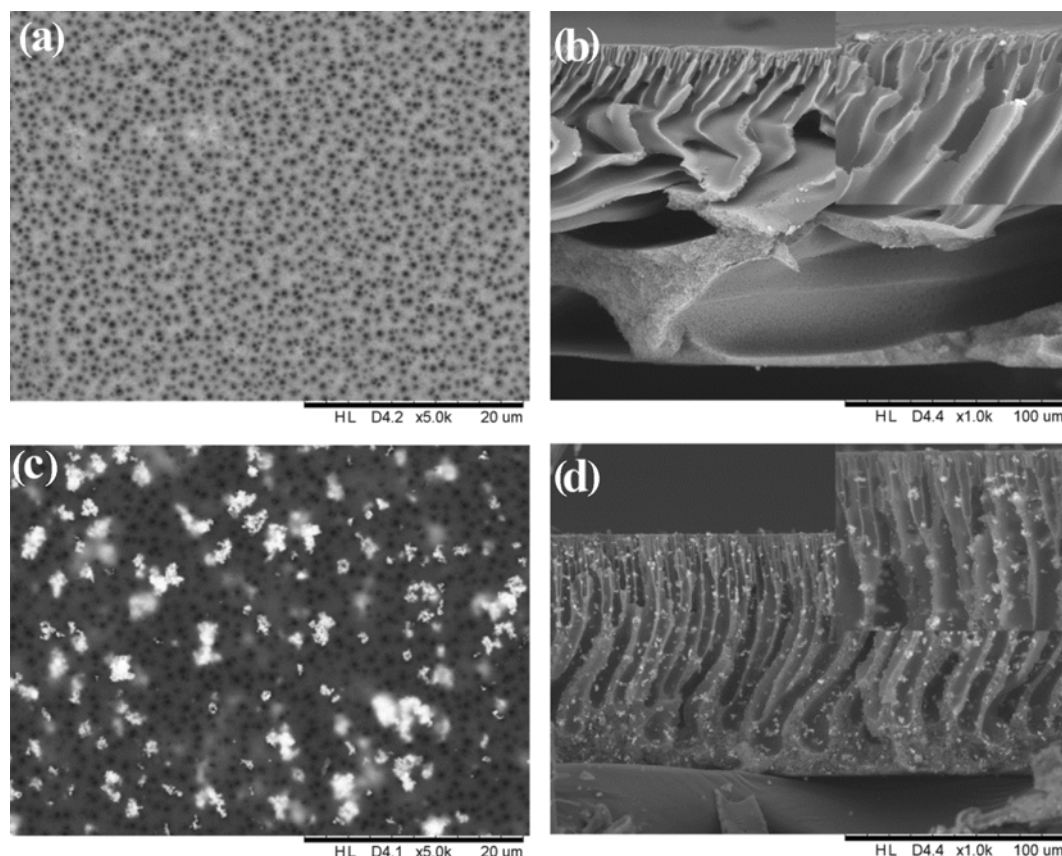Fig. 2. Experimental vs. predicted values of three responses (PWF, HAF and HAR).

Fig. 3. SEM images of run no. 15 ((a) surface, (b) cross section); run no. 9 ((c) surface, (d) cross section). The magnification of surface images is 5000×, while the magnification of cross sectional images is 1000× (the inset magnification is 3000×).
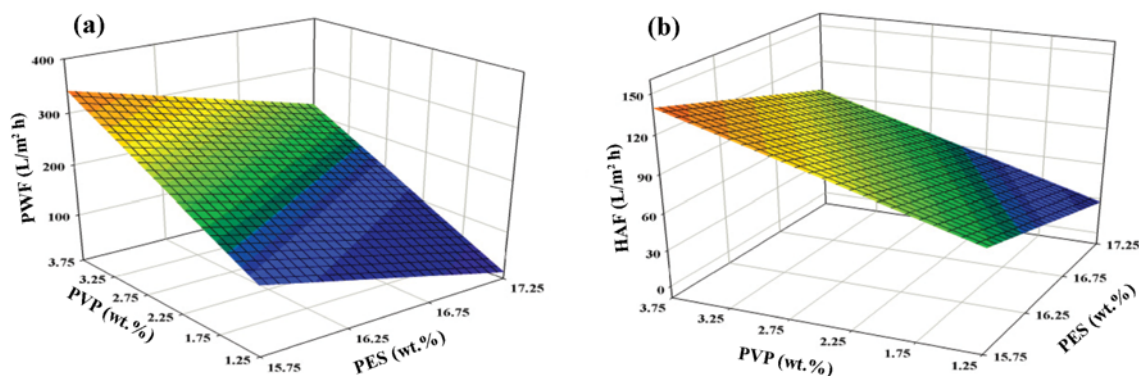

Fig. 4. The surface plot of PWF (a) and HAF (b) at different PES and PVP weight percentage (at 2.5 wt% of ZnO and 30 s of evaporation time).

the effect of both additives individually at the beginning. SEM images of run nos. 9 and 15 were plotted in Fig. 3 where, run no. 9 is dope-free of PVP, while run no.15 is dope-free of ZnO-NPs. It can be clearly seen from Fig. 3(a, b) that the membrane surface is highly porous (contain only PVP). There was also a finger-like structure with big macrovoids in the sub-layer and relatively porous skin layer.

The membrane that contained only ZnO-NPs as an additive had a less porous surface and there were clusters of nanoparticles aggregated on its surface (Fig. 3(c, d)). While, the cross section formed a finger-like structure along the membrane cross section

with skin layers at both sides of the membrane.

Fig. 4(a, b) shows the behavior of PWF and HAF in a three-dimensional surface plot; the ZnO and the evaporation time were fixed at 2.5 wt% and 30 s, respectively. The increase in PVP weight percentage and the decrease in PES weight percentage led to an increase in both PWF and HAF. It is generally accepted that the water permeability of the polymeric membranes increase with decrease in polymer concentration [39].

To illustrate the effect of PVP on membrane surface properties, the SEM graph of runs nos. 1 and 14 was plotted in Fig. 5. When PVP varied from 1.25 to 3.75 wt%, there was an increase in the
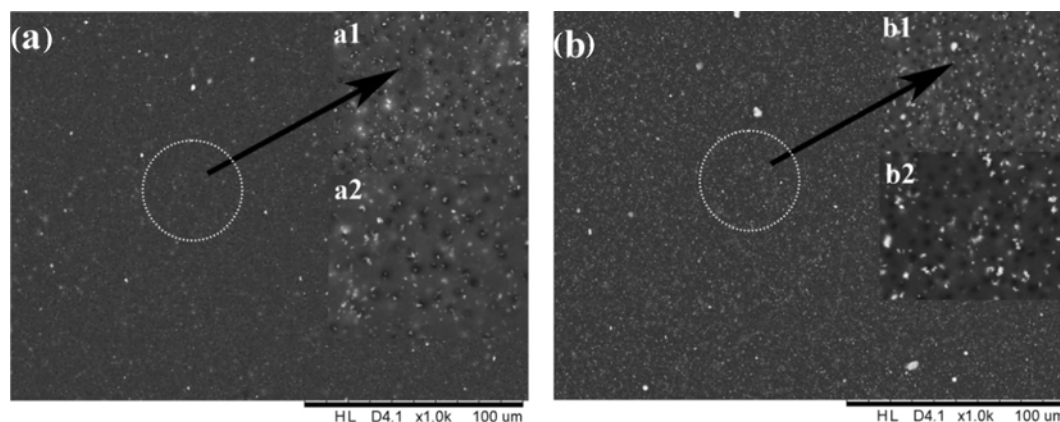
Fig. 5. SEM surface image of run no. 1-(a): (15.75 wt% PES; 1.25 wt% ZnO; 3.75 wt% PVP; 15 s time) and run no. 14-(b): (15.75 wt% PES; 1.25 wt% ZnO; 1.25 wt% PVP; 15 s time). The magnification of surface images ((a) and (b)) is 5000×, while the magnifications of the insets (a1 and b1) and (a2 and b2) are 3000× and 5000×, respectively.

apparent pore size. This result was expected because PVP is a well-known additive for pore formation, has the ability to increase viscosity, introduce hydrophilicity and improve pore formation [40]. This increase in the PVP content led to a more hydrophilic surface that attracts the water molecules. However, most of the PVP might be leached out during the filtration, but unfortunately, it is not easy to evaluate this leaching effect [34].

In addition to pore formation characteristic of PVP, it is also known to enhance the dispersion of ZnO-NPs and to increase the compatibility between the PES and the ZnO-NPs as displayed in Fig. 5(a). The enhancement in NPs dispersion rate led to an increase in the hydrophilic area that was exposed to water molecules. Thus, PWF and HAF were found to increase with PVP content due to increase in both pore size and surface hydrophilicity.

Hydrophilic ZnO-NPs was incorporated in the dope formulation to improve the membrane permeability as well as increase surface hydrophilicity. In our previous research [23], ZnO-NPs was added to PES polymer in the present of PVP to increase hydrophilicity and resulted to an increase in PWF as well as HAF. The increase in membrane flux in this case was attributed to the pore hydrophilization effect, as observed by Ngang et al. [41]. In this case, the NPs tends to form a hydroxyl group on the membrane surface and pore wall, which will induce more water to pass through the membrane. Vatanpour et al. [12] also found that 1 wt% of TiO_2 increases the PWF by 31.1% over 5% increase in membrane pore size. In contrast, it was believed that pore size plays the most important role in membrane flux improvement [42,43].

To understand the interaction effect between PES and ZnO-NPs on PWF response, their interaction was plotted in Fig. 6. At high ZnO content, there was an insignificant increase in PWF (from 120.43 to 177.48 L/m^2 h) with decrease in PES weight percentage. On the other hand, a significant increase in PWF (from 90.22 to 271.84 L/m^2 h) was observed at low ZnO content as PES tends to decrease. It is well known that the addition of ZnO-NP to a membrane polymeric solution can increase the solution's viscosity [23]. Fig. 7 explores the dope viscosity with different ZnO content at 15.75 and 17.25 weight percentages of PES polymer. At high ZnO-NPs content, the increase in PES weight percentage did
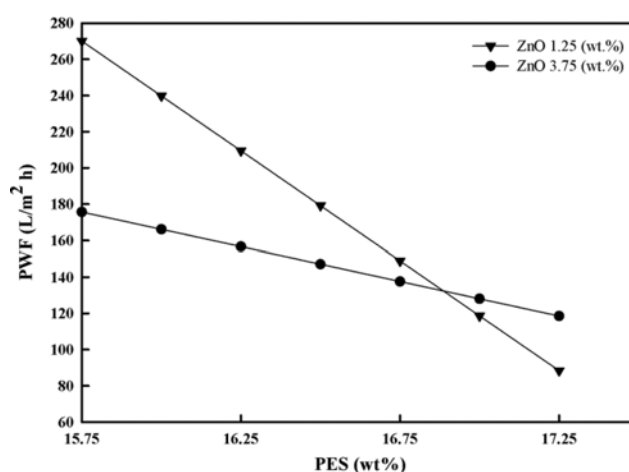

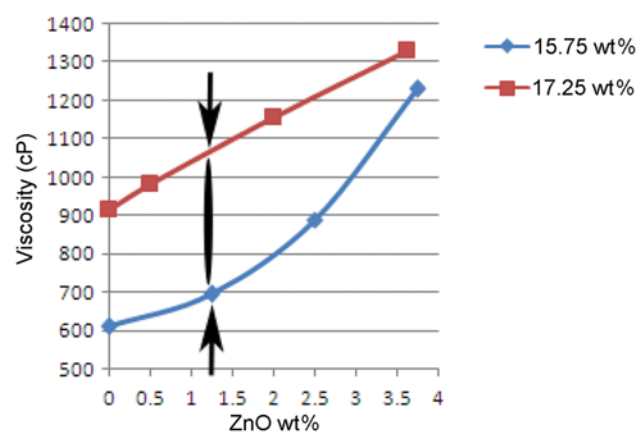**Fig. 6. Interaction effect between PES and ZnO-NPs weight percentages on PWF.**

Fig. 7. Variations in solution's viscosity with ZnO-NPs at two PES weight percentages.

not result in significant change in the solution's viscosity. However, at low ZnO-NPs weight percentage, the solution's viscosity was

changed significantly with PES polymer. Additionally, from Fig. 7, at 1.25 weight percentage of ZnO-NPs loading, the difference in the dope viscosities (at two PES weight percentages) reached a maximum limit.

The variation in PES/ZnO MM membrane morphology with dope viscosity was also reported elsewhere. For example, Shen et al. [19] found that the addition of ZnO-NPs to PES led to increase in dope viscosity. Moreover, at high amount of NPs loading (approximately 0.79 wt%), the viscosity effect dominated and led to a reduction in solvent-nonsolvent exchange rate, and subsequently reduced the membrane porosity. On the other hand, it was also found that the de-mixing will be delayed at higher dope viscosity, which led to produce a thicker inner skin of the hollow fiber membrane [44]. So, when the dope viscosity was reduced due to a decrease in PES concentration, the solvent-nonsolvent exchange rate was also expected to increase, thereby producing more porous structure and subsequently leading to an increase in PWF. Therefore, it can be concluded that the variation in dope viscosity resulted in a significant effect on PWF at low level of ZnO-NPs
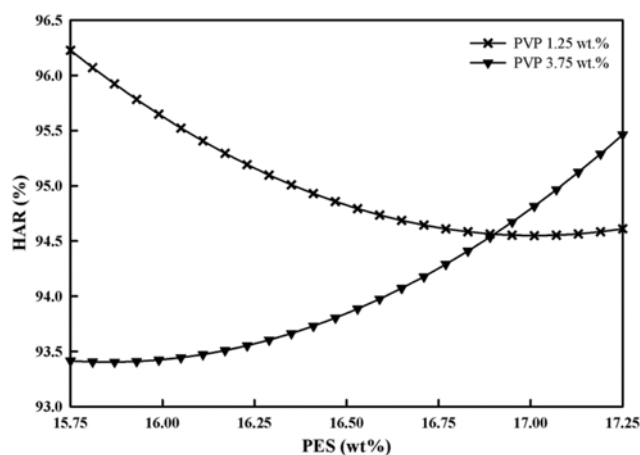
Fig. 9. Interaction effect between PES and PVP weight percentages (AC) for HAR.

(1.25 wt%).

3. HAR Response

The second-order term of solvent evaporation time (time^2) exhibited the most significant parameter in HAR model. To inspect the effect of this parameter, the SEM images of two similar dope formulations (runs no. 1 and 30) were selected according to their difference in the evaporation time (Fig. 8). As indicated in these images, the apparent pore size was reduced as the evaporation time increased by 30 s, as can be seen in Fig. 8(b). This phenomenon was also observed by other authors [45].

On the other hand, to investigate the effect of PES * PVP on HAR, the interaction between the PES and PVP weight percentages on the HAR at the central levels of ZnO-NPs and evaporation time was plotted in Fig. 9. At a low PVP weight percentage, an increase in the PES weight percentage decreases the membrane rejection. In this case, the amount of ZnO NPs was 2.5 wt%, and it was confirmed that the dispersion of NPs at low PVP content was poor, and therefore will negatively affect the membrane formation leading to bigger pore size as well as influence the membrane rejection. At high PVP weight percentages, there was an improvement in the membrane rejection as the PES weight percentage was increased. To inspect the NPs dispersion on membrane surface, the SEM surface of runs no. 13 and 2 was plotted in Fig. 10. The difference between the two images can be clearly spotted where the dispersion of nanoparticles was shown to improve at 3.75 weight percentage of PVP (Fig. 10(b)).

As a result, the presence of PVP at highest level (3.75 weight percentage) helped to improve both the pore formation and nanoparticles dispersion rate. Additionally, this also produced membrane with higher PWF and HAF due to an increase in both the apparent pore size and dispersion rate of the nanoparticles. However, introducing more PES to the solution would result in a membrane with a smaller pore size, thereby improving the HAR.

The effect of the PES and ZnO-NPs weight percentages on the HAR at the central level of PVP and evaporation time is shown in Fig. 11. As indicated, the HAR varies slightly with PES weight percentage and is shown to increase with ZnO-NPs weight percentage. This was obtained from ANOVA results (Table 3), in which
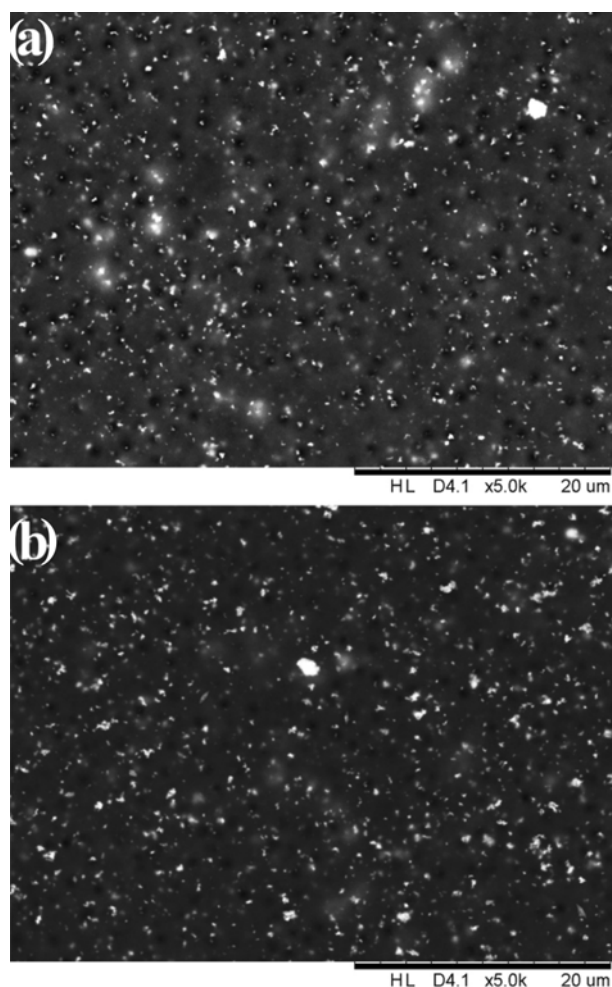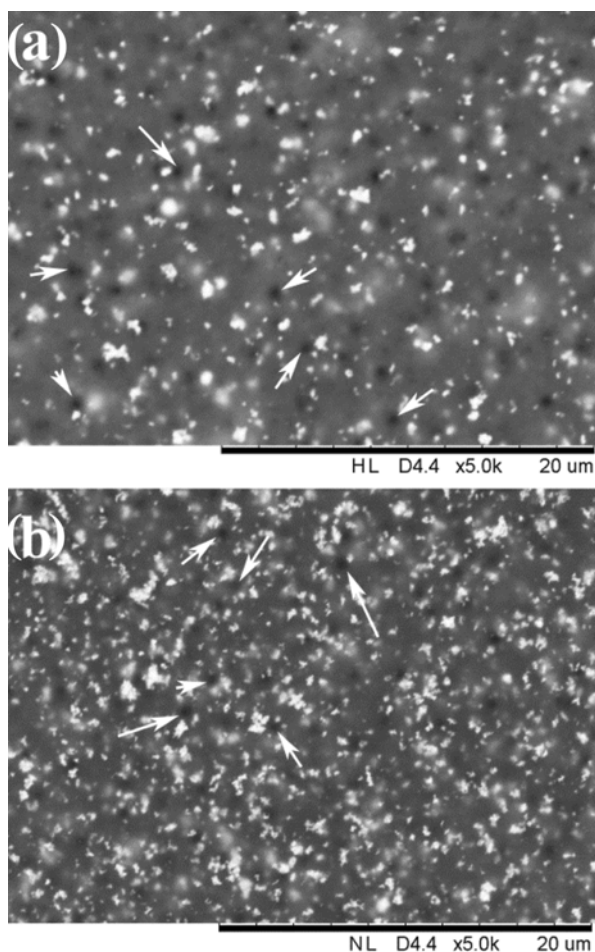

Fig. 8. SEM images of (a) - run no. 1 (a): (15.75 wt% PES; 1.25 wt% ZnO; 3.75 wt% PVP; 15 s time) and (b) - run no. 30 (b): (15.75 wt% PES; 1.25 wt% ZnO; 3.75 wt% PVP; 45 s time). The magnification of SEM images is 5000×.
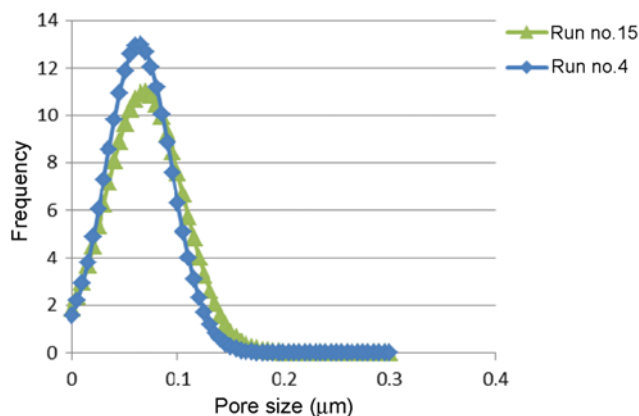
Fig. 12. Pore size distribution of run no. 15 (16.5 wt% PES; 0 wt% ZnO; 2.5 wt% PVP; 30 s time) and run no. 4 (16.5 wt% PES; 2.5 wt% ZnO; 2.5 wt% PVP; 30 s time).

the second-order term (B^2) showed significant model term for HAR. It was deduced from the previous discussion that the incorporation of ZnO-NPs to a polymeric membrane solution increases the solution's viscosity (Fig. 7). The viscosity effect precluded the exchange between the solvent and the non-solvent (water), leading to the formation of a membrane with smaller pores and a denser structure [46]. Thus, the incorporation of ZnO-NPs into the membrane structure improved the HAR. This result was further confirmed by measuring the pore size distribution of the membranes (runs no. 15 and 4) as shown in Fig. 12. Clearly, a tighter structure was obtained when 2.5 weight percentage of ZnO-NPs was added to the dope solution. However, when the ZnO-NPs weight percentage was increased to more than 3 weight percentage, the membrane rejection reduced slightly. This result might be due to the poor dispersion of the NPs at high weight percentages, resulting in a membrane with a bigger pore size that thereby affects the HAR. As a result from the previous analysis, the incorporation of ZnO-NPs into the membrane structure improved the HAR.

4. Optimization of the Membrane Preparation

It is important to find the optimum membrane preparation conditions. The purpose of the optimization process was to produce membranes with the maximum PWF, HAF and HAR. The software predicted that the optimized conditions (at a desirability of 0.75) for PWF, HAF and HAR were obtained when the PES, ZnO-NPs, PVP weight percentages and evaporation time were 17.25 wt%, 3.62 wt%, 3.75 wt%, and 15 s, respectively. Under these conditions, the predicted PWF, HAF and HAR were 222.3 (L/m^2 h), 94.7 (L/m^2 h), and 96.4%, respectively. The predicted responses (PWF, HAF and HAR) were compared with the actual responses to investigate the percentage of error. The percentage of error was calculated using Eq. (4):

$$\text{Error (\%)} = \left(\frac{\text{Actual value - Predicted value}}{\text{Actual value}} \right) * 100\% \qquad (4)$$

Table 4 shows the confirmation runs for the experimental and predicted responses with the percentage of error for each response. From this investigation, the membrane formula along with the

Fig. 10. SEM surface graph (a)-run no. 13 (15.75 wt% PES; 3.75 wt% ZnO; 1.25 wt% PVP; 45 s time) and (b)-run no. 2 (15.75 wt% PES; 3.75 wt% ZnO; 3.75 wt% PVP; 45 s time). The magnification of surface images is 5000×.
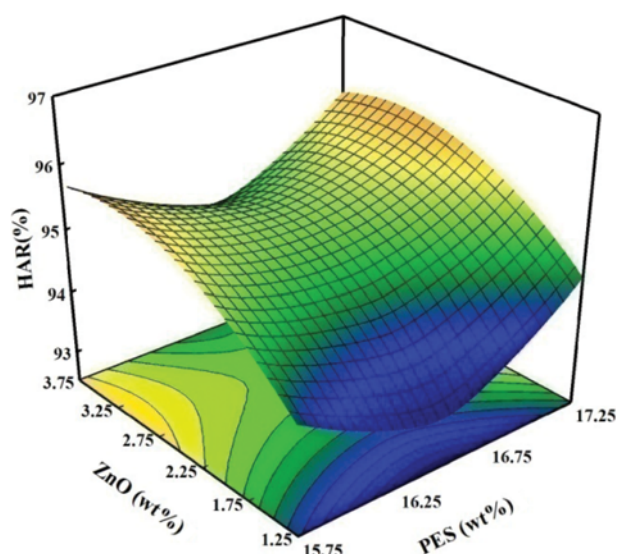

Fig. 11. The surface plot for the HAR at different PES and ZnO-NPs weight percentage (at 2.5 wt% of PVP and 30 s of evaporation time).

Table 4. Predicted and experimental optimum values of the PWF, HAF and HAR

	PWF (L/m² h)	Error (%)	HAF (L/m² h)	Error (%)	HAR (%)	Error (%)
Predicted	222.30	-	94.7	-	96.34	-
Run1	190.00	−17.00	115	17.65	98.13	1.82
Run 2	259.00	14.17	120	21.08	95.19	−1.21
Run 3	267.00	16.74	122	22.38	97.05	0.73
Average of runs	238.67	6.86	119	20.42	96.79	0.46

evaporation time can be optimized and used to improve the PWF, HAF and HAR. The percentage of error reflects the variations between the experimental and the predicted values and cannot be avoided.

CONCLUSIONS

RSM was employed in the design of these experiments and to optimize the preparation conditions of PES/ZnO mixed matrix membranes. The synthetic parameters were the PES, ZnO-NPs, PVP weight percentages and the solvent evaporation time. Three quadratic models were developed to correlate the preparation variables to the three responses (PWF, HAF and HAR). The following conclusions can be drawn:

• PES and PVP weight percentages were found to have a significant effect on PWF and HAF responses. Also, the presence of PVP in dope solution improved both pore formation as well as the NPs dispersion rate. PWF and HAF were found to increase with PVP content due to increase in pore size and surface hydrophilicity (as a result of improved NPs dispersion rate). The interaction effect between PES and ZnO-NPs (A∗B) showed a significant effect on PWF in which the dope viscosity was found to be a dominant factor especially at low ZnO-NPs. At this level of NPs loading (1.25 wt%), the improvement in PWF with a reduction in PES weight percentage were attributed to significant decrease in dope viscosity.

• The quadratic effects of solvent evaporation time and ZnO-NPs weight percentage in addition with the interacting effect between PES and PVP weight percentage resulted as the most significant parameters that affects HAR. It was observed that the increase in evaporation time affects HAR positively; however, this parameter shows insignificant effect on PWF and HAF. Furthermore, an increase in PES weight percentage at high level of PVP (3.75 wt%) resulted in a membrane with smaller pore size, thus improving the HAR.

• The optimum preparation conditions for mixed matrix membrane were 17.25 wt%, 3.62 wt%, 3.75 wt% and 15 s for the PES, ZnO-NPs, PVP weight percentages and solvent evaporation time, respectively. Under these conditions, the predicted PWF, HAF and HAR were 222.3 (L/m² h), 94.7 (L/m² h) and 96.34%, respectively.

ACKNOWLEDGEMENTS

REFERENCES

1. P. C. Singer, *Water Sci. Technol.*, **40**, 25 (1999).
2. N. A. A. Sani, W. J. Lau and A. F. Ismail, *Korean J. Chem. Eng.*, **32**, 743 (2015).
3. A. Salahi, T. Mohammadi, R. M. Behbahani and M. Hemmati, *Korean J. Chem. Eng.*, **32**, 1101 (2015).
4. A. L. Ahmad, A. A. Abdulkarim, B. S. Ooi and S. Ismail, *Chem. Eng. J.*, **223**, 246 (2013).
5. M. S. Muhamad, M. R. Salim and W.-J. Lau, *Korean J. Chem. Eng.*, **32**(11), 2319 (2015).
6. J. H. Kim and C. K. Kim, *J. Membr. Sci.*, **262**, 60 (2005).
7. L.-F. Han, Z.-L. Xu, Y. Cao, Y.-M. Wei and H.-T. Xu, *J. Membr. Sci.*, **372**, 154 (2011).
8. F. Ran, S. Nie, W. Zhao, J. Li, B. Su, S. Sun and C. Zhao, *Acta Biomater.*, **7**, 3370 (2011).
9. J. Huang, J. Xue, K. Xiang, X. Zhang, C. Cheng, S. Sun and C. Zhao, *Colloids Surf., B*, **88**, 315 (2011).
10. A. Rahimpour, S. S. Madaeni and Y. Mansourpanah, *Desalination*, **258**, 79 (2010).
11. J.-J. Qin, M. H. Oo and Y. Li, *J. Membr. Sci.*, **247**, 119 (2005).
12. V. Vatanpour, S. S. Madaeni, A. R. Khataee, E. Salehi, S. Zinadini and H. A. Monfared, *Desalination*, **292**, 19 (2012).
13. S. Balta, A. Sotto, P. Luis, L. Benea, B. Van der Bruggen and J. Kim, *J. Membr. Sci.*, **389**, 155 (2012).
14. N. Maximous, G. Nakhla, W. Wan and K. Wong, *J. Membr. Sci.*, **352**, 222 (2010).
15. F. Liu, N. A. Hashim, Y. Liu, M. R. M. Abed and K. Li, *J. Membr. Sci.*, **375**, 1 (2011).
16. J. F. Hernández-Sierra, F. Ruiz, D. C. Cruz Pena, F. Martínez-Gutiérrez, A. E. Martínez, A. de Jesús Pozos Guillén, H. Tapia-Pérez and G. Martínez Castañón, *Nanomed. Nanotechnol. Biol. Med.*, **4**, 237 (2008).
17. A. Dodd, A. McKinley, M. Saunders and T. Tsuzuki, *J. Nanopart. Res.*, **8**, 43 (2006).
18. Y. Wang, L. Yang, G. Luo and Y. Dai, *Chem. Eng. J.*, **146**, 6 (2009).
19. L. Shen, X. Bian, X. Lu, L. Shi, Z. Liu, L. Chen, Z. Hou and K. Fan, *Desalination*, **293**, 21 (2012).
20. S. Anitha, B. Brabu, D. J. Thiruvadigal, C. Gopalakrishnan and T. S. Natarajan, *Carbohydr. Polym.*, **87**, 1065 (2012).
21. H. Bai, Z. Liu and D. D. Sun, *Colloids Surf., A*, **410**, 11 (2012).
22. C. Leo, W. Cathie Lee, A. Ahmad and A. Mohammad, *Sep. Purif. Technol.*, **89**, 51 (2012).
23. A. L. Ahmad, A. A. Abdulkarim, S. Ismail and B. S. Ooi, *Desalin. Water Treat.*, **54**, 3257 (2015).
24. Y. Lan, P. Peng and B. Shi, *Sep. Sci. Technol.*, **46**, 2211 (2011).

25. A. F. Ismail and P. Lai, *Sep. Purifi. Technol.*, **40**, 191 (2004).

26. Y. Ma, Y. Zhang, S. Zhao, Y. Wang, S. Wang, Y. Zhou, N. Li, H. Xie, W. Yu and Y. Liu, *J. Biomed. Mat. Res. Part A*, **100**, 989 (2012).

27. G. Bakeri, A. F. Ismail, D. Rana, T. Matsuura and M. Shariaty, *J. Appl. Polymer Sci.*, **123,** 2812 (2012).

28. L. Y. Ng, C. P. Leo and A. W. Mohammad, *J. Appl. Polymer Sci.*, **121**, 1804 (2011).

29. M. A. Ahmad, W. M. H. F. W. Harun, N. K. A. Rashid, A. L. Ahmad, O. Sidek, M. Afif, M. Miskam, J. Ramli, A. Hadi and A. Jeefferie, *Int. J. Eng. Technol.*, **10**, 1 (2010).

30. K. Anand, S. Varghese and T. Kurian, *Powder Technol.*, **271**, 187 (2015).

31. I. M. Mahbubul, R. Saidur, M. A. Amalina, E. B. Elcioglu and T. Okutucu-Ozyurt, *Ultrason. Sonochem.*, **26**, 361 (2015).

32. A. Khan, J. Shang and R. Alam, *Int. J. Environ. Sci. Technol.*, **11**, 1989 (2014).

33. W. Subramonian, T. Y. Wu and S.-P. Chai, *Ind. Crops Prod.*, **70**, 107 (2015).

34. J. Ahmad and M. B. Hågg, *J. Membr. Sci.*, **445**, 200 (2013).

35. A. Mendonza, J. Warzywoda and A. Sacco, Jr., *J. Porous Mater.*, **13**, 37 (2006).

36. C. S. Goh, H. T. Tan, K. T. Lee and A. R. Mohamed, *Fuel Process. Technol.*, **91**, 1146 (2010).

37. K. P. Y. Shak and T. Y. Wu, *Ind. Crops Prod.*, **76**, 1169 (2015).

38. S. Rajesh, S. Senthilkumar, A. Jayalakshmi, M. T. Nirmala, A. F. Ismail and D. Mohan, *Colloids Surf., A*, **418**, 92 (2013).

39. B. Vatsha, J. C. Ngila and R. M. Moutloali, *Phys. Chem. Earth., Parts A/B/C*, **67-69**, 125 (2014).

40. Y. Liu, G. H. Koops and H. Strathmann, *J. Membr. Sci.*, **223**, 187 (2003).

41. H. P. Ngang, B. S. Ooi, A. L. Ahmad and S. O. Lai, *Chem. Eng. J.*, **197**, 359 (2012).

42. A. Razmjou, J. Mansouri and V. Chen, *J. Membr. Sci.*, **378**, 73 (2011).

43. J.-F. Li, Z.-L. Xu, H. Yang, L.-Y. Yu and M. Liu, *Appl. Surf. Sci.*, **255**, 4725 (2009).

44. L. Wang, Z. Li, J. Ren, S.-G. Li and C. Jiang, *J. Membr. Sci.*, **275**, 46 (2006).

45. D. B. Mosqueda-Jimenez, R. M. Narbaitz, T. Matsuura, G. Chowdhury, G. Pleizier and J. P. Santerre, *J. Membr. Sci.*, **231**, 209 (2004).

46. H. Ohya, S. Shiki and H. Kawakami, *J. Membr. Sci.*, **326**, 293 (2009).